Pulmonary Effects of Sustained Periods of High-G Acceleration Relevant to Suborbital Spaceflight

Ross D. Pollock; Caroline J. Jolley; Nadia Abid; John H. Couper; Luis Estrada-Petrocelli; Peter D. Hodkinson; Steffen Leonhardt; Snapper Magor-Elliott; Tobias Menden; Gerrard Rafferty; Graham Richmond; Peter A. Robbins; Grant A. D. Ritchie; Mitchell J. Segal; Alec T. Stevenson; Henry D. Tank; Thomas G. Smith

BACKGROUND: Members of the public will soon be taking commercial suborbital spaceflights with significant $+G_x$ (chest-to-back) acceleration potentially reaching up to $+6\ G_x$. Pulmonary physiology is gravity-dependent and is likely to be affected, which may have clinical implications for medically susceptible individuals.

METHODS: During 2-min centrifuge exposures ranging up to $+6\ G_x$, 11 healthy subjects were studied using advanced respiratory techniques. These sustained exposures were intended to allow characterization of the underlying pulmonary response and did not replicate actual suborbital G profiles. Regional distribution of ventilation in the lungs was determined using electrical impedance tomography. Neural respiratory drive (from diaphragm electromyography) and work of breathing (from transdiaphragmatic pressures) were obtained via nasoesophageal catheters. Arterial blood gases were measured in a subset of subjects. Measurements were conducted while breathing air and breathing 15% oxygen to simulate anticipated cabin pressurization conditions.

RESULTS: Acceleration caused hypoxemia that worsened with increasing magnitude and duration of $+G_x$. Minimum arterial oxygen saturation at $+6\ G_x$ was 86 ± 1% breathing air and 79 ± 1% breathing 15% oxygen. With increasing $+G_x$ the alveolar-arterial (A-a) oxygen gradient widened progressively and the relative distribution of ventilation reversed from posterior to anterior lung regions with substantial gas-trapping anteriorly. Severe breathlessness accompanied large progressive increases in work of breathing and neural respiratory drive.

DISCUSSION: Sustained high-G acceleration at magnitudes relevant to suborbital flight profoundly affects respiratory physiology. These effects may become clinically important in the most medically susceptible passengers, in whom the potential role of centrifuge-based preflight evaluation requires further investigation.

KEYWORDS: $+G_x$ acceleration, commercial suborbital spaceflight, space travel, respiratory physiology, hypoxemia, passenger health.

Pollock RD, Jolley CJ, Abid N, Couper JH, Estrada-Petrocelli L, Hodkinson PD, Leonhardt S, Mago-Elliott S, Menden T, Rafferty G, Richmond G, Robbins PA, Ritchie GAD, Segal MJ, Stevenson AT, Tank HD, Smith TG. *Pulmonary effects of sustained periods of high-G acceleration relevant to suborbital spaceflight*. Aerosp Med Hum Perform. 2021; 92(7):633–641.

Private citizens will soon be flying on commercial suborbital spaceflights.[38] As at the dawn of air travel a century ago, suborbital flights will not be widely affordable initially, but high-speed suborbital spaceflight is ultimately expected to revolutionize global transportation by transforming long-haul routes into short trips (e.g., London–New York in 30 min).[29]

Current suborbital flights provide several minutes of weightlessness. This is preceded and followed by short periods of high acceleration (high 'G forces' or 'G') during launch and atmospheric re-entry that are potentially greater in magnitude than

From King's College London, London, United Kingdom; the University of Oxford, Oxford, United Kingdom; the Barcelona Institute of Science and Technology, Barcelona, Spain; RWTH Aachen University, Aachen, Germany; and QinetiQ, Farnborough, Hampshire, United Kingdom.

This manuscript was received for review in September 2020. It was accepted for publication in March 2021.

Address correspondence to: Thomas G. Smith, M.B.B.S., D.Av.Med., D.Phil., FRCA, FAsMA, Head of Aerospace Medicine Research, Centre for Human and Applied Physiological Sciences, Shepherd's House, Guy's Campus, London SE1 1UL, United Kingdom; thomas.g.smith@kcl.ac.uk.

DOI: https://doi.org/10.3357/amhp.5790.2021

for NASA's now-retired Space Shuttle, although shorter in duration (typically less than a minute).[1,6,9] Unlike professional astronauts, suborbital passengers may have widely varying age, fitness, and baseline health—hundreds of people have already purchased flights, including many who are elderly (some older than 90 yr of age) or have significant medical problems, or both. The physiological and clinical implications of this dynamic flight environment in such a diverse population have yet to be established.[1,8] According to U.S. regulations, commercial spaceflight crew must demonstrate an ability to withstand the stresses of spaceflight, including high acceleration, but there is no regulatory requirement for centrifuge-based training or experience for prospective suborbital passengers.[8,38]

Spacecraft occupants are usually reclined in a supine position during launch and re-entry phases so that acceleration is experienced in the chest-to-back direction (+G_x). This reduces the likelihood of loss of consciousness compared with the head-to-foot direction when seated upright (+G_z, experienced by fast-jet pilots), but instead causes chest compression that has been commonly likened to an 'elephant sitting on the chest'.[19] Anticipated suborbital G loads may exceed +3 G_x for periods of 20–30 s, reaching a transient peak of up to +6 G_x on re-entry.[6,9] At +6 G_x an object's weight is increased sixfold so that, for example, an 85-kg person weighs half a ton.

Most individuals with well-controlled medical conditions are expected to be capable of safely tolerating the hypergravity phases of suborbital spaceflight.[8] Centrifuge-simulated suborbital acceleration profiles conducted under normoxic conditions have been tolerated by many volunteers of widely varying ages and with minor and stable medical conditions,[7,9,10] although physical symptoms and problematic anxiety were quite common and approximately 5% of volunteers were unable to complete the exposures, possibly related in part to a sensation of difficulty breathing.[8,26] Limited measurements of arterial oxygen saturation (S_pO_2) in some individuals indicated desaturation as low as 89% that was not associated with adverse sequelae.[9,10] Pulmonary physiology has not otherwise been studied during simulated suborbital profiles, yet the lung is unusually vulnerable to gravitational effects—it has little actual tissue mass and deforms under its own weight.[31]

The precise role of gravity and its interaction with other factors in lung physiology is not completely understood, but postural effects of gravity on respiratory function are well established in clinical medicine, such as the use of prone positioning in critically ill patients.[18,25] Regional ventilation and blood flow normally increase toward the dependent region of the lung, but become more inhomogeneous with increasing high G acceleration, eventually resulting in hypoxemia secondary to ventilation/perfusion mismatch.[16,17,31] Perfusion of the nondependent lung is reduced[16,17] while compression of lung tissue under its increased weight, further compounded by the displacement of mediastinal contents, leads to airway closure within dependent lung regions, loss of alveolar ventilation, and shunt.[5,28,31] Centrifuge studies primarily conducted in healthy subjects in the 1960s[3,16,28] and more recently[5,31,32] have induced well-tolerated hypoxemia using various magnitudes and durations of +G_x acceleration.[17] Based on extrapolation from these diverse studies it is possible that hypoxemia may occur during suborbital flights. This would not necessarily be clinically concerning in itself, particularly in individuals who are young and healthy, but may have greater significance in older and less healthy individuals.

Such hypoxemia could be exacerbated by the use of airline-style cabin pressurization on suborbital spacecraft. Commercial airline passengers routinely experience mild hypoxia (S_pO_2 typically 90–95%) due to reduced atmospheric pressure within the cabin that is equivalent to an altitude of up to 8000 ft (2438 m).[2] This is sufficient to activate classic physiological responses to hypoxia in flight such as erythropoietin secretion and hypoxic pulmonary vasoconstriction.[36,39] More severe hypoxemia occurs in passengers with respiratory disease and in some healthy individuals, particularly with increasing age, and can contribute to adverse medical events in flight.[2,27,34] Some suborbital spacecraft will have similarly reduced cabin pressure and thus similarly hypoxic conditions, which in theory could accentuate any G-induced hypoxemia and impact medically susceptible individuals,[1] but this has not yet been investigated.

This study aimed to characterize the underlying pulmonary response to +G_x acceleration in order to guide the medical approach to prospective suborbital flyers and improve passenger safety. Rather than replicate the brief and dynamic G profiles of actual suborbital flights, this study used sustained G exposures to allow more complete and detailed characterization of the underlying pulmonary response. We aimed to determine how +G_x acceleration loads ranging up to +6 G_x affect respiratory physiology, what degree of hypoxemia this may cause, and how this is influenced by simulated airline-style cabin pressurization.

METHODS

Subjects

Healthy volunteers were recruited following medical screening, which included a health questionnaire, medical examination, 12-lead ECG, urinalysis, and spirometry. Detailed inclusion and exclusion criteria are described in the supplementary online appendix (**Appendix A**; https://doi.org/10.3357/AMHP.5790sd.2021) together with further details of the experimental methods. The study was approved by the King's College London and QinetiQ Research Ethics Committees and was conducted in accordance with the Declaration of Helsinki. All subjects provided written informed consent. There were 11 healthy subjects who took part in the study, which used a randomized, repeated measures, crossover design.

Equipment

The study was undertaken using a long-arm human centrifuge (radius 9.14 m; QinetiQ, Farnborough, UK). Heart rate (from three-lead ECG), S_pO_2 at the earlobe, and tidal volume and respiratory rate (from a pneumotachograph in line with the demand valve regulator controlling breathing gas delivery) were recorded continuously via Powerlab 16SP and LabChart 7 (AD

Instruments, Oxford, UK). Breath-by-breath end-tidal partial pressures of oxygen ($P_{ET}O_2$) and carbon dioxide ($P_{ET}CO_2$) were measured using an in-line molecular flow sensor (University of Oxford, Oxford, UK).[13]

Regional distribution of lung ventilation was determined using electrical impedance tomography (EIT) via 16 circumferential chest electrodes (Goe-MF II EIT device, CareFusion, Höchberg, Germany).[15] This technique uses bio-impedance measurements in which a sinusoidal current is injected and the resulting surface potential measured in adjacent electrodes. Through these measurements, EIT tracks lung conductivity as it varies depending on the degree of inflation and forms a tomographic image that reflects regional ventilation. EIT is used in respiratory research and is under investigation for clinical use. Functional EIT images at each acceleration level were used in eight regions of interest in the lung defined as anterior (A1–A4) and posterior (P1–P4) moving from chest to back. Tidal impedance and end-expiratory impedance were determined and normalized to a percentage of global impedance for each region of interest (Dräger EIT Data Analysis Tool 6.1, Dräger Medical, Lübeck, Germany).[15]

In nine subjects, nasoesophageal catheters were used to study respiratory drive to the diaphragm (neural respiratory drive) and breathing mechanics. Diaphragm electromyography (EMG_{di}) was recorded continuously from an esophageal multipair electrode catheter and expressed as a proportion of the value obtained during maximum volitional inspiratory maneuvers (EMG_{di}%max) as previously described.[21] EMG_{di}%max was multiplied by respiratory rate to calculate the neural respiratory drive index (NRDI; arbitrary units, AU).[21,23] Transdiaphragmatic pressure was measured simultaneously using a dual pressure transducer tipped catheter (Gaeltec, Dunvegan, UK) with the proximal transducer in the midesophagus and the distal transducer in the stomach, and the diaphragm pressure-time product (PTP_{di}) was calculated to provide an index of the work of breathing.[4,22]

Arterial blood gases were analyzed in a subset of three subjects via a 20-gauge radial artery cannula. Subjects withdrew an arterial sample immediately prior to completing each G exposure. A video and description of the arterial sampling procedure on the centrifuge are included in the supplementary online appendix (Appendix A; https://doi.org/10.3357/AMHP.5790sd.2021). The

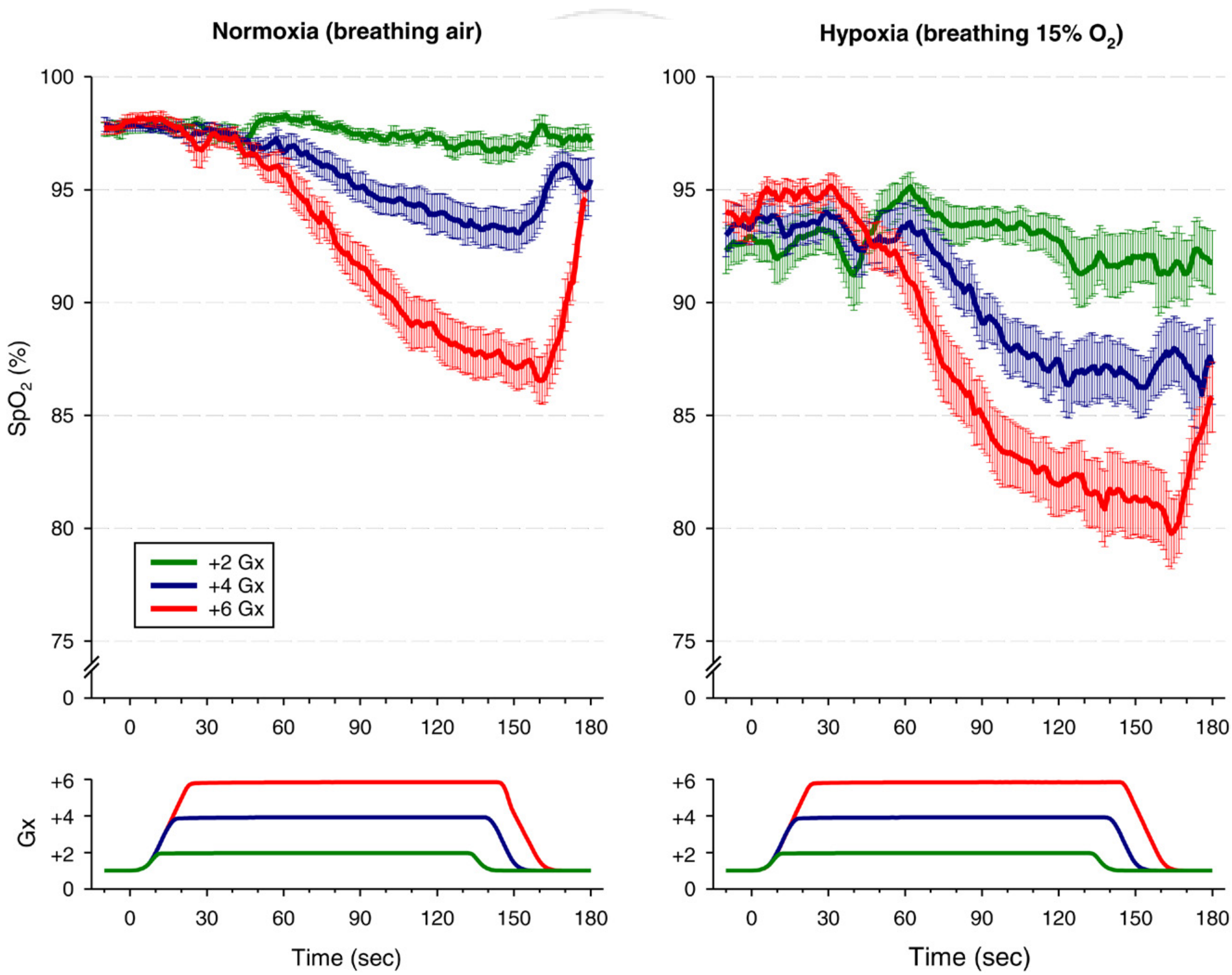

Fig. 1. Arterial oxygen saturation during $+G_x$ acceleration Upper panels show arterial oxygen saturation (S_pO_2) and lower panels show applied acceleration (G_x). Left panels show measurements breathing air and right panels show measurements breathing 15% oxygen to simulate a cabin pressure altitude of 8000 ft (2438 m). Data are mean ± SEM.

alveolar-arterial (A-a) gradient was calculated using the alveolar gas equation, with an assumed *R* value of 0.8.

Procedure

Subjects wore comfortable clothes with no anti-G trousers or other G protection. Following instrumentation subjects were positioned supine in the centrifuge gondola wearing an occlusive nose clip and breathing through a mouthpiece. Exposures of 2 min to +2, +4, and +6 G_x were undertaken twice, once breathing air and once breathing 15% oxygen (balance 85% nitrogen) to simulate a cabin pressure altitude of 8000 ft (2438 m).[2] The order of exposures was randomized and subjects were

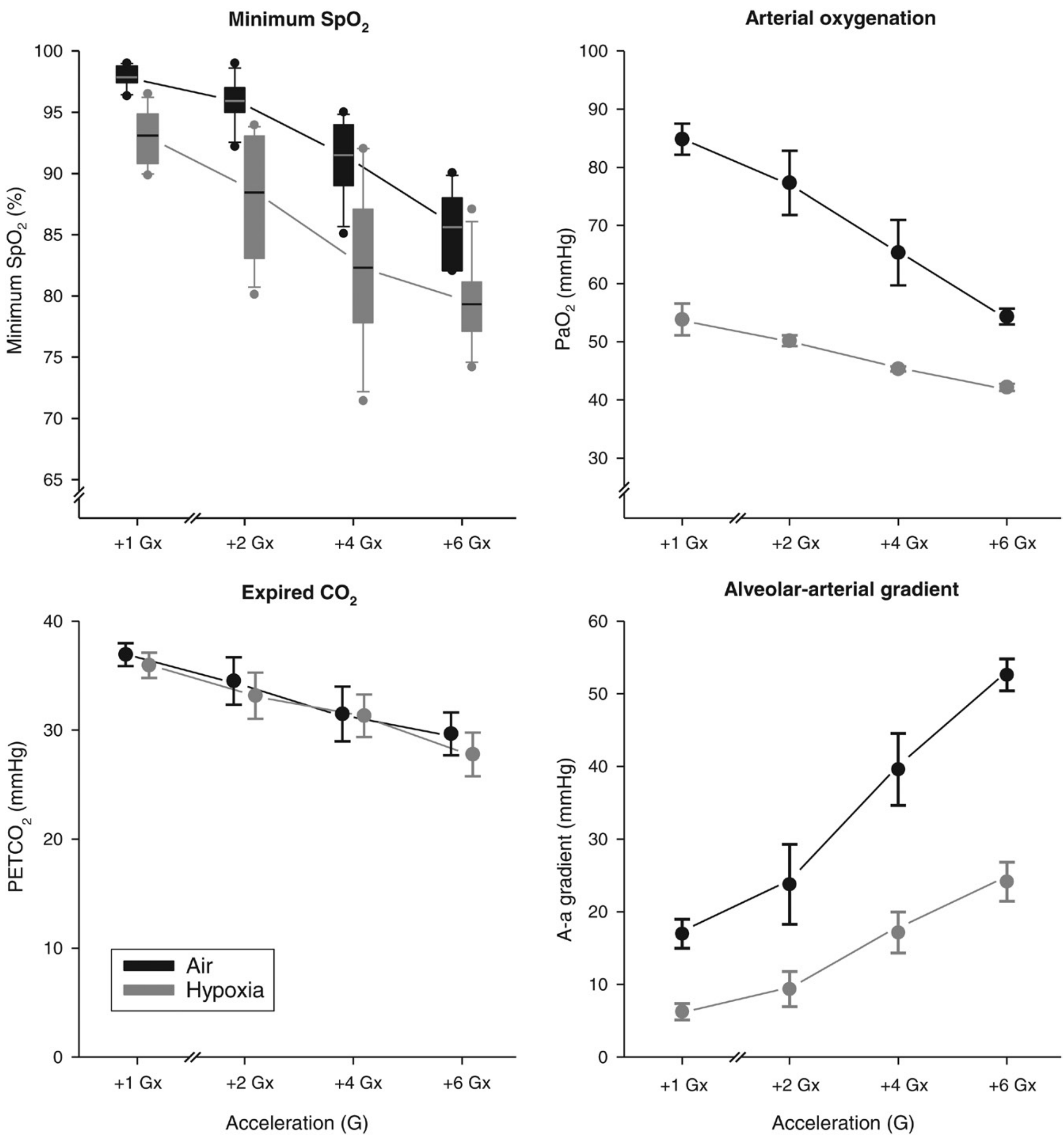

Fig. 2. Pulmonary gas exchange during $+G_x$ acceleration. Upper left panel shows the minimum arterial oxygen saturation (S_pO_2) observed during each G exposure, including the mean, interquartile range (boxes), 10–90% range (bars), and individual outliers beyond this range. Upper right panel shows the arterial partial pressure of oxygen (P_aO_2), lower right panel shows the calculated alveolar-arterial (A-a) oxygen gradient, and lower left panel shows the end-tidal partial pressure of carbon dioxide ($P_{ET}CO_2$); data are mean ± SEM. Data were obtained while breathing air (black symbols) and breathing 15% oxygen to simulate a cabin pressure altitude of 8000 ft (2438 m; gray symbols).

blinded to the gas mixture. The centrifuge was stationary for at least 5 min between exposures. Breathlessness intensity was recorded using the modified Borg (mBorg) scale[11] and subjects were asked to report any symptoms of pain or discomfort.

Statistical Analysis

The study was powered to detect a change in S_pO_2 of 5 percentage points with a power of 80% and a two-sided significance of 0.05. Statistical analysis was conducted using IBM SPSS Statistics and statistical significance was assumed at $P < 0.05$. Data were normally distributed (Shapiro-Wilk test). Differences between G levels and breathing gases were assessed using one-way and two-way repeated measures ANOVA with Greenhouse-Geisser correction and with Bonferroni adjustment for multiple comparisons. Data are reported as mean ± SEM unless otherwise stated.

RESULTS

There were 11 subjects (8 men and 3 women) with mean (± SD) age 29 ± 6 yr, weight 80 ± 17 kg, height 1.76 ± 0.09 m, and body mass index 26 ± 4 ($kg \cdot m^{-2}$). There was a large fall in S_pO_2 during exposure to $+G_x$ acceleration (**Fig. 1** and **Fig. 2**), indicating substantial impairment of gas exchange. The fall in S_pO_2 increased significantly with the magnitude [$F(1.7,13.4) = 19.3$, $P < 0.001$] and duration [$F(1.5,12.2) = 26.9$, $P < 0.001$] of $+G_x$, reaching a minimum S_pO_2 of 86 ± 1% at +6 G_x while breathing air. Breathing 15% oxygen significantly exacerbated these effects [$F(1,8) = 64.7$, $P < 0.001$], with a minimum S_pO_2 of 79 ± 1% at +6 G_x (Fig. 2). These effects were evident even at +2 G_x (minimum S_pO_2 96 ± 1% breathing air and 88 ± 1% breathing 15% oxygen).

Similarly, the arterial partial pressure of oxygen (P_aO_2) fell with increasing $+G_x$ to 54 ± 1 mmHg at +6 G_x [$F(1.9,3.8) = 15.9$, $P = 0.015$] and was significantly lower breathing 15% oxygen [$F(1,2) = 69.8$, $P = 0.014$], reaching 42 ± 1 mmHg at +6 G_x (Fig. 2). The A-a gradient widened substantially with increasing acceleration to a peak of 53 ± 2 mmHg at +6 G_x [$F(1.5,3.0) = 38.4$, $P = 0.008$; Fig. 2], indicating worsening impairment of ventilation/perfusion matching. The A-a gradient was smaller with reduced inspired oxygen [$F(1,2) = 76.7$, $P = 0.013$], but still widened with increasing $+G_x$ (Fig. 2). $P_{ET}CO_2$ fell with increasing $+G_x$ [$F(1.9,13.5) = 17.4$, $P < 0.001$], but was not significantly affected by inspired oxygen level [$F(1,7) = 5.4$, $P = 0.053$; Fig. 2]. Changes in $P_{ET}O_2$ (Fig. A2 online) and heart rate (Fig. A3 online) are reported in the supplementary online Appendix A (https://doi.org/10.3357/AMHP.5790sd.2021).

With increasing acceleration from +1 G_x baseline to +6 G_x there was a reversal of the normal relative distribution of ventilation from posterior to anterior lung regions. A progressive inversion of normalized tidal impedance from chest to back and a significant interaction between region of interest and G level [$F(4.0,35.9) = 10.8$, $P < 0.001$; **Fig. 3**] were observed. End-expiratory impedance increased in the most anterior lung regions with increasing $+G_x$, with a significant interaction between region of interest and G level [$F(3.4,30.3) = 11.9$, $P < 0.001$], indicating higher end-expiratory regional lung volume due to progressively greater gas-trapping anteriorly (Fig. 3).

Increasing acceleration loads caused a substantial, dose-dependent increase in the work of breathing, with PTP_{di} increasing from 242 ± 22 $cmH_2O \cdot s^{-1} \cdot min^{-1}$ at baseline to 658 ± 86 $cmH_2O \cdot s^{-1} \cdot min^{-1}$ at +6 G_x when breathing air [$F(1.3,10.3) = 36.8$, $P < 0.001$; **Fig. 4**]. A parallel increase from baseline to +6 G_x in EMG_{di}%max (11 ± 1% vs. 45 ± 7%) and in NRDI [112 ± 14 AU vs. 825 ± 174 AU, $F(1.1,8.6) = 17.0$, $P = 0.003$; Fig. 4] was observed. Whereas NRDI, PTP_{di} and respiratory rate [$F(2.1,20.8) = 34.4$, $P < 0.001$; Fig. 4] increased with increasing $+G_x$, tidal volume decreased significantly [$F(2.7,27.4) = 9.7$, $P < 0.001$; Fig. 4], limiting the consequent increase in ventilation [$F(1.7,16.9) = 11.1$, $P = 0.001$; Fig. 4]. Thus, increasing $+G_x$ was associated with progressive neuroventilatory uncoupling (i.e., increased neural respiratory drive without a parallel increase in ventilation)[20] [further depicted in **Fig. A4** and **Fig. A5** in the supplementary online appendix (Appendix A; https://doi.org/10.3357/AMHP.5790sd.2021)]. Breathing 15% oxygen resulted in greater increases in PTP_{di} [$F(1,8) = 38.8$, $P < 0.001$], but had no further significant effects on NRDI [$F(1,8) = 4.3$, $P = 0.072$] or the other ventilatory parameters (Fig. 4).

Subjectively, subjects reported increasing breathlessness with each step change in acceleration [$F(1.3,12.8) = 64.1$, $P < 0.001$], with severe breathlessness at +6 G_x (median mBorg 5 [IQR 3.5-7]), and mildly hypoxic conditions resulted in further increases in mBorg [$F(1,10) = 6.3$, $P = 0.031$; Fig. 4]. Eight subjects (73%) reported musculoskeletal chest pain at +4 or +6 G_x, which was generally parasternal or subcostal and worse on inspiration, and persisted for 2 d after testing in two subjects.

DISCUSSION

Currently there are no medical criteria for determining an individual's suitability for suborbital spaceflight, reflecting the lack of evidence on which to base such criteria.[38] While most people are likely to be able to tolerate a suborbital spaceflight safely,[8] a deeper understanding of the underlying physiology may assist medical decision-making for individuals with conditions that raise particular concerns. This study has demonstrated that sustained periods of $+G_x$ at magnitudes relevant to suborbital spaceflight profoundly affect respiratory physiology and impair gas exchange in healthy individuals. Marked hypoxemia and breathlessness were exacerbated by simulating potential cabin pressure conditions with mild hypoxia, although mean S_pO_2 did not fall below 85% within the first minute, which is most relevant to actual suborbital flights.

Conducting detailed physiological measurements during high-G acceleration is complex, challenging, and rarely attempted, and the integration of multiple advanced techniques is a strength of this study. To our knowledge, no previous centrifuge studies have used electrical impedance tomography, diaphragm electromyography, esophageal/gastric manometry, molecular flow sensing, or concurrent hypoxia during $+G_x$ acceleration. A

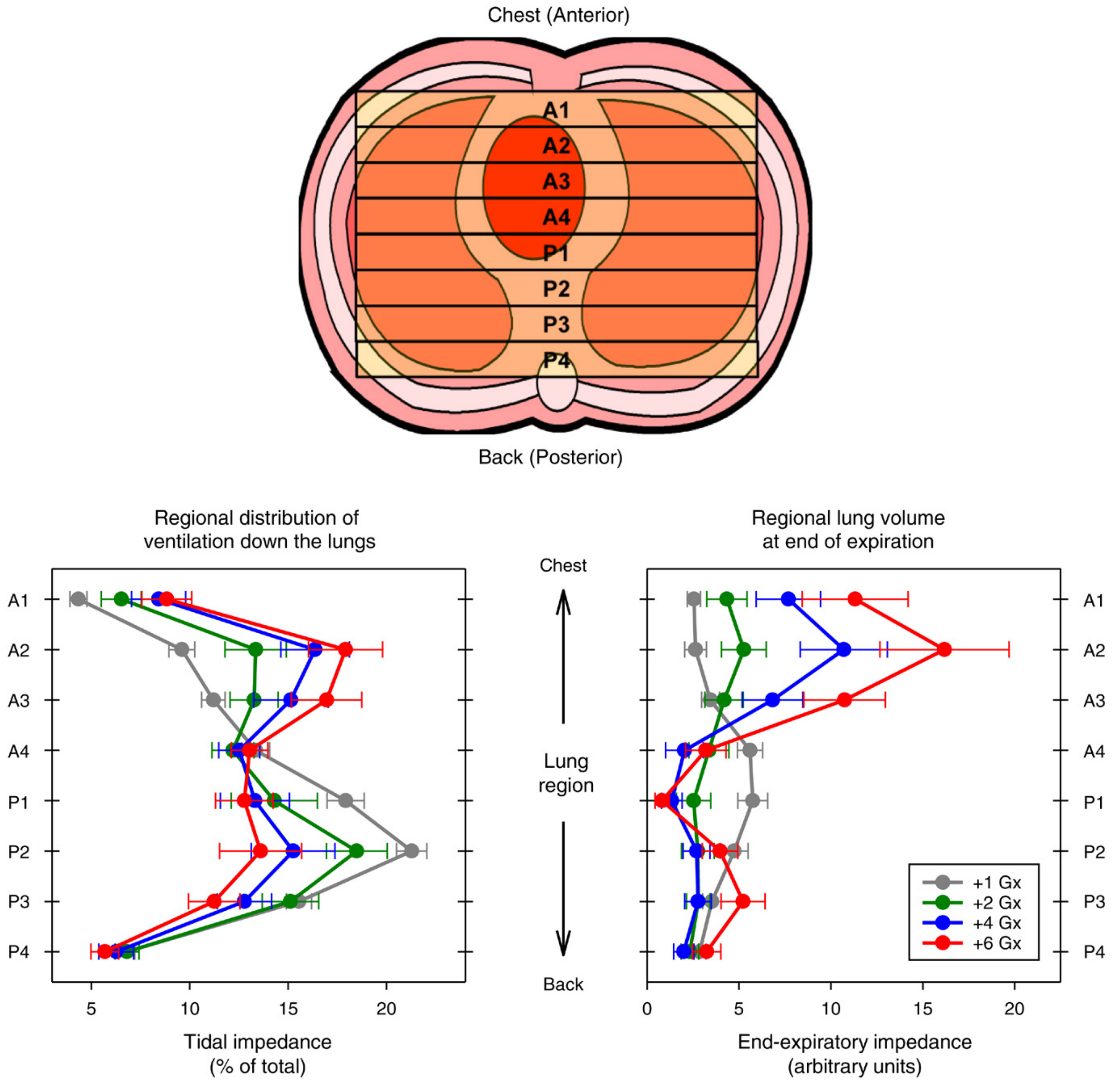

Fig. 3. Regional distribution of ventilation in the lungs during +G_x acceleration. Electrical impedance was averaged in eight regions of interest in the lung defined as anterior (A1–A4) and posterior (P1–P4) moving from chest to back (illustrated in upper panel). Lower left panel shows the regional distribution in tidal ventilation derived from tidal impedance expressed as a percentage of global impedance. Lower right panel shows the regional lung volume at the end of expiration derived from end-expiratory impedance. Data are mean ± SEM.

limitation of the study is that the physiology of young healthy subjects does not necessarily reflect that of older age groups, with associated higher prevalence of medical disease that may be more characteristic of commercial spaceflight participants,[8] at least for early flights. In this respect the current study is only a starting point and detailed physiological studies in more representative subjects are still required.

This study did not seek to replicate the anticipated G profiles of actual suborbital flights in which in-flight acceleration peaks and overall G exposures will be brief compared with the sustained G required to characterize the underlying pulmonary response. As such, the responses we observed are not expected to be evident generally in suborbital passengers, but rather provide an understanding of the physiological processes that will be triggered and may interact with individual factors such as pre-existing morbidity. On actual flights the in-flight +G_x exposure may also be intensified by a simultaneous +G_z component in some circumstances (e.g., seated crew),[9] and the period of microgravity could itself interfere with gas exchange in the elderly or in the presence of lung pathology.[24,35] Furthermore, rapid transition to high G from zero G (rather than from 1 G, as in the current study) could impair tolerance during actual

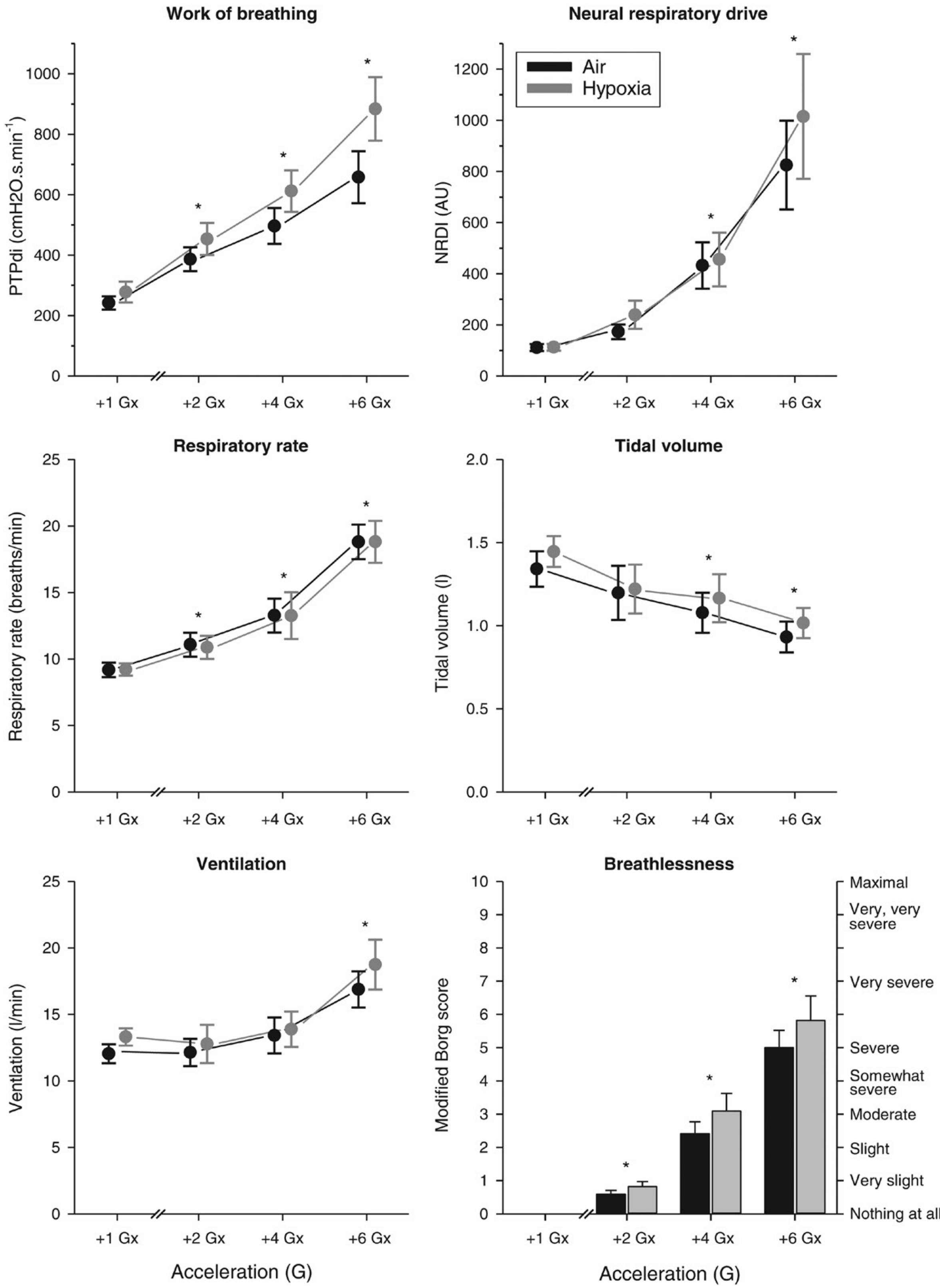

Fig. 4. Breathing mechanics, breathing drive, ventilation, and breathlessness during $+G_x$ acceleration. Work of breathing was determined from transdiaphragmatic pressure as the diaphragm pressure-time product (PTPdi). Neural respiratory drive index (NRDI) was determined from diaphragm electromyography (EMG_{di}) as the proportion of maximum volitional EMG_{di} ($EMGdi_{\%max}$) multiplied by respiratory rate. Breathlessness intensity was rated using the modified Borg scale. Data were obtained while breathing air (black symbols) and breathing 15% oxygen to simulate a cabin pressure altitude of 8000 ft (2438 m; gray symbols). Asterisks denote a statistically significant difference ($P < 0.05$) from baseline for respective G loads after Bonferroni adjustment for multiple comparisons. Data are mean ± SEM.

suborbital re-entry, when peak $+G_x$ is sufficient to make it momentarily difficult even to move.[1]

This study found that magnitudes of $+G_x$ acceleration experienced over the suborbital range profoundly changed the regional distribution of pulmonary ventilation and the mechanical behavior of the lung and chest wall. Progressive anterior gas-trapping combined (in real-time) with a relative reversal in regional lung ventilation has not been identified with previous techniques.[5,16] With increasing $+G_x$ the ventilatory response was limited by impaired pulmonary mechanics leading to neuroventilatory uncoupling and disproportionate breathlessness.[20,33] These are novel data. The peak values observed for work of breathing and neural respiratory drive were higher than those typically seen in patients with severe chronic obstructive pulmonary disease[21] or obesity.[37] Indeed, together with the pronounced anterior gas-trapping, the effect of increasing $+G_x$ was analogous to a transient form of respiratory failure associated with such disease states. High-G acceleration also multiplies body weight and suborbital profiles can be considered as briefly inducing a temporary 'super obesity-like' state that, like obesity itself, causes respiratory embarrassment.[37]

Although transitory, such respiratory compromise raises potential concerns for individuals who are already obese or have lung pathology, with greater potential to contribute to adverse clinical sequelae such as cardiac events (e.g., malignant rhythms or myocardial infarction[12]) or parenchymal lung damage.[40] Suborbital G exposures will be considerable for an untrained population, although they are likely to be physically tolerable for most younger healthy people. For others, the extent to which suborbital flights may evoke the underlying responses reported in this study will depend on interaction with individual factors such as age, body mass, smoking history, baseline fitness, and pre-existing disease.

Suborbital spaceflight is ultimately expected to become commonplace as a means of transportation and overcoming potential respiratory challenges will help to enable as many people as possible to fly safely. Possible protective strategies for at-risk individuals include supplementary oxygen, continuous positive airway pressure (CPAP), and centrifuge-based evaluation and training. However, increasing the inspired concentration of oxygen is unlikely to reverse the hypoxemia completely and is complicated in high G due to the phenomenon of acceleration atelectasis, whereby the consequent reduction in 'nitrogen-splinting' of alveoli encourages their collapse.[30] Unobtrusive CPAP devices used routinely in managing obstructive sleep apnea could directly oppose the effects of $+G_x$ acceleration and warrant investigation for use in medically susceptible individuals with relevant conditions.[37]

For individuals in whom there is the greatest potential for adverse effects, centrifuge-based evaluation prior to suborbital spaceflight may be particularly beneficial and informative. A 'G challenge test' could be employed much like a hypoxic challenge test (breathing 15% oxygen) is used to predict in-flight responses in vulnerable airline passengers.[14] The G challenge test could consist of continuous monitoring of S_pO_2 and heart rate (as a minimum), together with subjective measures (breathlessness, discomfort, anxiety), during graded-intensity suborbital G profiles. This could be combined with simultaneous hypoxia breathing 15% oxygen, with countermeasures (such as CPAP) and with additional training activities. Studies are required to investigate the potential role for such testing in evaluating individuals with specific medical concerns such as comorbid cardiorespiratory illness and obesity. In the meantime, we suggest it may be prudent to consider centrifuge-based evaluation as part of the medical assessment in these circumstances.

In conclusion, this study demonstrates that sustained periods of high-G acceleration relevant to commercial suborbital spaceflight profoundly affect respiratory physiology, causing substantial hypoxemia and breathlessness that are exacerbated by simulated cabin pressure conditions. These effects are not expected to be clinically meaningful for the majority of spaceflight participants, but provide a deeper understanding of the physiological processes that will be triggered during suborbital flight and that may impact on a minority of individuals. Further research is required to determine whether centrifuge-based testing can improve medical evaluation prior to suborbital flight for the most medically susceptible individuals, with the aim of optimizing passenger health while maximizing access to suborbital spaceflight.

ACKNOWLEDGMENTS

The authors thank Dr. Jeremy Radcliffe, Dr. Des Connolly, and the centrifuge staff for assistance with experiments, Karl-Heinz Fromm for assistance with processing EIT files, and the volunteers for taking part in this study. The authors also acknowledge the very extensive contribution of the Farnborough centrifuge to acceleration research over its lifetime (1955-2019).

Financial Disclosure Statement: This work was supported by a grant from the UK Space Agency (ST/R006113/1). The authors have no competing interests to declare.

Authors and Affiliations: Ross D. Pollock, Ph.D., Caroline J. Jolley, MRCP, Ph.D., Nadia Abid, M.B.B.S., M.Sc., Peter D. Hodkinson, MRCP, Ph.D., Gerrard Rafferty, Ph.D., Mitchell J. Segal, M.Sc., and Thomas G. Smith, M.B.B.S., D.Phil., D.Av.Med., FRCA, FAsMA, King's College London, London, United Kingdom; John H. Couper, Snapper Magor-Elliott, M.A., Graham Richmond, Ph.D., Peter A. Robbins, BMBCh, D.Phil., and Grant A. D. Ritchie, D.Phil., University of Oxford, Oxford, United Kingdom; Lius Estrada-Petrocelli, Ph.D., Barcelona Institute of Science and Technology, Barcelona, Spain; Steffen Leonhardt, M.D., Ph.D., and Tobias Menden, M.Sc., RWTH Aachen University, Aachen, Germany; and Alec T. Stevenson, Ph.D., and Henry D. Tank, M.Sc., QinetiQ, Farnborough, Hampshire, United Kingdom; Thomas G. Smith, M.B.B.S., D.Phil., D.Av.Med., FRCA, FAsMA, Guy's and St. Thomas' NHS Foundation Trust, London, United Kingdom.

REFERENCES

1. Aerospace Medical Association Commercial Spaceflight Working Group. Suborbital commercial spaceflight crewmember medical issues. Aviat Space Environ Med. 2011; 82(4):475–484.
2. Ahmedzai S, Balfour-Lynn IM, Bewick T, Buchdahl R, Coker RK, et al. Managing passengers with stable respiratory disease planning air travel: British Thoracic Society recommendations. Thorax. 2011; 66(Suppl. 1):i1–i30.

3. Alexander WC, Sever RJ, Hoppin FG Jr. Hypoxemia induced in man by sustained forward acceleration while breathing pure oxygen in a five pounds per square inch absolute environment. Aerosp Med. 1966; 37(4):372–378.
4. American Thoracic Society/European Respiratory Society. ATS/ERS statement on respiratory muscle testing. Am J Respir Crit Care Med. 2002; 166(4):518–624.
5. Ax M, Karlsson LL, Sanchez-Crespo A, Lindahl SG, Linnarsson D, et al. Regional lung ventilation in humans during hypergravity studied with quantitative SPECT. Respir Physiol Neurobiol. 2013; 189(3):558–564.
6. Blue Origin. New Shepard Payload User's Guide (Revision E). Kent (WA): Blue Origin; 2018.
7. Blue RS, Bonato F, Seaton K, Bubka A, Vardiman JL, et al. The effects of training on anxiety and task performance in simulated suborbital spaceflight. Aerosp Med Hum Perform. 2017; 88(7):641–650.
8. Blue RS, Jennings RT, Antunano MJ, Mathers CH. Commercial spaceflight: progress and challenges in expanding human access to space. REACH. 2017; 7–8:6–13.
9. Blue RS, Pattarini JM, Reyes DP, Mulcahy RA, Garbino A, et al. Tolerance of centrifuge-simulated suborbital spaceflight by medical condition. Aviat Space Environ Med. 2014; 85(7):721–729.
10. Blue RS, Riccitello JM, Tizard J, Hamilton RJ, Vanderploeg JM. Commercial spaceflight participant G-force tolerance during centrifuge-simulated suborbital flight. Aviat Space Environ Med. 2012; 83(10):929–934.
11. Borg GA. Psychophysical bases of perceived exertion. Med Sci Sports Exerc. 1982; 14(5):377–381.
12. Cayce WR, Zerull RG. Myocardial infarction occurring at the conclusion of centrifuge training in a 37-year-old aviator. Aviat Space Environ Med. 1992; 63(12):1106–1108.
13. Ciaffoni L, O'Neill DP, Couper JH, Ritchie GA, Hancock G, Robbins PA. In-airway molecular flow sensing: a new technology for continuous, noninvasive monitoring of oxygen consumption in critical care. Sci Adv. 2016; 2(8):e1600560.
14. Dine CJ, Kreider ME. Hypoxia altitude simulation test. Chest. 2008; 133(4):1002–1005.
15. Frerichs I, Amato MB, van Kaam AH, Tingay DG, Zhao Z, et al. Chest electrical impedance tomography examination, data analysis, terminology, clinical use and recommendations: consensus statement of the TRanslational EIT developmeNt stuDy group. Thorax. 2017; 72(1):83–93.
16. Glaister DH. Distribution of pulmonary blood flow and ventilation during forward (+Gx) acceleration. J Appl Physiol. 1970; 29(4):432–439.
17. Glaister DH. The effects of gravity and acceleration on the lung. AGARDograph 133. England: Technivision Services; 1970.
18. Guérin C, Reignier J, Richard JC, Beuret P, Gacouin A, et al. Prone positioning in severe acute respiratory distress syndrome. N Engl J Med. 2013; 368(23):2159–2168.
19. Hall L. Got a ticket to space? You'll have to train first. Air Space. 2017; 2017(June):43–47.
20. Jolley CJ, Luo YM, Steier J, Rafferty GF, Polkey MI, Moxham J. Neural respiratory drive and breathlessness in COPD. Eur Respir J. 2015; 45(2):355–364.
21. Jolley CJ, Luo YM, Steier J, Reilly C, Seymour J, et al. Neural respiratory drive in healthy subjects and in COPD. Eur Respir J. 2009; 33(2):289–297.
22. Laveneziana P, Albuquerque A, Aliverti A, Babb T, Barreiro E, et al. ERS statement on respiratory muscle testing at rest and during exercise. Eur Respir J. 2019; 53(6):1801214.
23. Luo YM, Moxham J. Measurement of neural respiratory drive in patients with COPD. Respir Physiol Neurobiol. 2005; 146(2–3):165–174.
24. Mackenzie I, Viirre E, Vanderploeg JM, Chilvers ER. Zero G in a patient with advanced amyotrophic lateral sclerosis. Lancet. 2007; 370(9587):566.
25. McNicholas B, Cosgrave D, Giacomini C, Brennan A, Laffey JG. Prone positioning in COVID-19 acute respiratory failure: just do it? Br J Anaesth. 2020; 125(4):440–443.
26. Mulcahy RA, Blue RS, Vardiman JL, Mathers CH, Castleberry TL, Vanderploeg JM. Subject anxiety and psychological considerations for centrifuge-simulated suborbital spaceflight. Aviat Space Environ Med. 2014; 85(8):847–851.
27. Naughton MT, Rochford PD, Pretto JJ, Pierce RJ, Cain NF, Irving LB. Is normobaric simulation of hypobaric hypoxia accurate in chronic airflow limitation? Am J Respir Crit Care Med. 1995; 152(6, Pt. 1):1956–1960.
28. Nolan AC, Marshall HW, Cronin L, Sutterer WF, Wood EH. Decreases in arterial oxygen saturation and associated changes in pressures and roentgenographic appearance of the throax during forward (+Gx) acceleration. Aerosp Med. 1963; 34:797–813.
29. Peeters W. A roadmap for suborbital commercial passenger spaceflight. New Space. 2013; 1(2):81–90.
30. Pollock RD, Gates SD, Storey JA, Radcliffe JJ, Stevenson AT. Indices of acceleration atelectasis and the effect of hypergravity duration on its development. Exp Physiol. 2021; 106(1):18–27.
31. Prisk GK. Gas exchange under altered gravitational stress. Compr Physiol. 2011; 1(1):339–355.
32. Rohdin M, Petersson J, Mure M, Glenny RW, Lindahl SG, Linnarsson D. Protective effect of prone posture against hypergravity-induced arterial hypoxaemia in humans. J Physiol. 2003; 548(Pt. 2):585–591.
33. Scano G, Innocenti-Bruni G, Stendardi L. Do obstructive and restrictive lung diseases share common underlying mechanisms of breathlessness? Respir Med. 2010; 104(7):925–933.
34. Smith TG, Chang RW, Robbins PA, Dorrington KL. Commercial air travel and in-flight pulmonary hypertension. Aviat Space Environ Med. 2013; 84(1):65–67.
35. Smith TG, Formenti F, Hodkinson PD, Khpal M, Mackenwells BP, Talbot NP. Monitoring tissue oxygen saturation in microgravity on parabolic flights. Gravit Space Res. 2016; 4(2):2–7.
36. Smith TG, Talbot NP, Chang RW, Wilkinson E, Nickol AH, et al. Pulmonary artery pressure increases during commercial air travel in healthy passengers. Aviat Space Environ Med. 2012; 83(7):673–676.
37. Steier J, Jolley CJ, Seymour J, Roughton M, Polkey MI, Moxham J. Neural respiratory drive in obesity. Thorax. 2009; 64(8):719–725.
38. Stepanek J, Blue RS, Parazynski S. Space medicine in the era of civilian spaceflight. N Engl J Med. 2019; 380(11):1053–1060.
39. Turner BE, Hodkinson PD, Timperley AC, Smith TG. Pulmonary artery pressure response to simulated air travel in a hypobaric chamber. Aerosp Med Hum Perform. 2015; 86(6):529–534.
40. Wood EH. Potential hazards of high anti-Gz suit protection. Aviat Space Environ Med. 1992; 63(11):1024–1026.

APPENDIX A.

Author Contributions

T. G. Smith conceived and designed the study. R. D. Pollock, C. J. Jolley, S. Leonhardt, T. Menden, P. A. Robbins, and A. T. Stevenson contributed to the study design. All authors acquired, analyzed, or interpreted the data. T. G. Smith drafted the manuscript. All authors were responsible for critical revision of the manuscript for important intellectual content.

SUPPLEMENTARY METHODS

Inclusion/Exclusion Criteria

Inclusion criteria for subjects:

- Ages 18–55 yr inclusive and in good health.

Exclusion criteria for subjects:

- Any history of cardiovascular disease (including, but not limited to, postural hypotension, hypertension, varicosities, echocardiogram abnormalities, any right ventricular dysfunction, significant asymptomatic aortic stenosis, clinically significant regurgitant valvular disease, structural ventricular abnormalities, ECG abnormalities, venous thrombosis, congestive cardiac failure, congenital heart disease, cardiac surgery, or myocardial infarction);
- Any history of chronic or acute upper or lower respiratory disease (including asthma, spontaneous pneumothorax, chronic obstructive airways disease, cystic fibrosis, emphysema, or other respiratory condition);
- Any history of neurological disorder (including epilepsy, any form of unexplained loss of consciousness, serious head injury, congenital or acquired neurological defect, transient ischemic attacks, or severe migraine);
- Any active back or neck pain or symptoms suggesting nerve root compression or history of significant past/current back or neck injury or pathology;
- Any history of significant peripheral arterial or venous vascular disease including giant cell arteritis, varicose veins, deep venous thrombosis, hemorrhoids, or arterio-venous malformations;
- Any history of diabetes mellitus or any significant endocrine disturbance (including current conditions for which the subject is taking medication);
- Any history of unexplained visual disturbance, retinal detachment, or retinal vascular disease, especially central/branch retinal artery/vein occlusion;
- Anemia from any cause and sickle cell trait;
- Any use of drugs promoting lowered blood pressure or motion sickness;
- Any other medical condition considered unacceptable to the Medical Officer; or
- Pregnancy.

Further exclusion criteria for use of esophageal catheters:

- Recent midfacial (including nasal) or upper gastro-intestinal tract trauma or surgery;
- Abnormal esophageal anatomy for example presence of strictures or diverticula, tracheoesophageal fistula, esophageal varices; or
- Coagulopathy or history of recurrent or significant epistaxis.

Further exclusion criteria for arterial cannulation:

- History of vascular injury or ischemia of the arms (such as frostbite, cold injury, Raynaud's syndrome/phenomenon).

Further Experimental Methods

Subjects were required to avoid alcohol and strenuous exercise for 12 h prior to the experimental visit, and to refrain from caffeine intake 2 h prior to the centrifuge exposures. Female subjects were asked to confirm that they were not pregnant at the time of the study and undertook a urine pregnancy test.

On arrival at the centrifuge facility, the subject's fitness to undergo centrifuge exposure was confirmed by a medical officer. For those subjects in whom arterial sampling was undertaken, a 20-gauge arterial cannula was inserted in the radial artery under local anesthetic (subcutaneous bleb of lidocaine 1%) using an aseptic technique. Before entering the gondola, subjects were instrumented with:

- 3-lead ECG electrodes;
- 16 electrical impedance tomography electrodes around the chest (see **Fig. A1**); and
- esophageal catheters inserted under local anesthetic (topical spray to the nasopharynx).

Following instrumentation subjects were positioned supine in the centrifuge gondola wearing an occlusive nose clip and breathing through a mouthpiece. Breathing gases were supplied to the subject using an aircraft oxygen regulator to ensure consistent breathing system characteristics across the two gas conditions. The breathing circuit incorporated a pneumotachograph (allowing measurement of inspiratory volumes) and an in-line molecular flow sensor (University of Oxford, Oxford, UK). Once positioned in the gondola the measurement equipment was connected and the centrifuge harness was secured without compromising the ability to make maximal ventilatory efforts. A forced vital capacity maneuver was performed at baseline and during the first seconds at each G plateau. Acceleration to and from each G level plateau was achieved at an onset/offset rate of $0.3\ G \cdot s^{-1}$. Communication was via audio (two-way) and video monitoring of subjects, who used hand signals to communicate when breathing through the mouthpiece.

Photographs and video footage in this supplementary appendix were taken and reproduced with the consent of subjects and investigators.

Measurements via Esophageal Catheters

Measurements. Transdiaphragmatic pressure (P_{di}) was measured as the difference between gastric and esophageal pressure obtained using a dual pressure transducer tipped catheter (CTO-2; Gaeltec Devices Ltd, Dunvegan, UK) and associated amplifer (S7d; Gaeltec Devices Ltd), as previously described.[1,10,12] Crural EMG_{di} was recorded using a multipair esophageal electrode catheter (Yinghui Medical Equipment Technology Co. Ltd, Guangzhou, China). The catheter consisted of nine consecutive recording electrode coils, which formed five pairs of electrodes.[5,7] The pressure transducer and electrode catheters were inserted transnasally using nasopharyngeal local anesthetic (lidocaine) spray. Once correctly positioned they were taped to the nose to prevent movement during the study. Due to technical limitations, during the centrifuge runs, EMG_{di} signals were recorded from electrode pairs 1, 2, 4, and 5 only. The EMG_{di} signals were amplified (gain 100) and band-pass filtered between 10–2000 Hz before acquisition (CED 1902; Cambridge Electronic Design Limited, Cambridge, UK). All signals were acquired using a 16-bit analog-to-digital converter (PowerLab 16/35; ADInstruments Ltd, Oxford, UK) and displayed on a laptop computer running LabChart software (Version 7.2, ADInstruments Pty, Colorado Springs, CO, USA) with analog to digital sampling at 100 Hz (flow and pressures), and 4000 Hz ($oesEMG_{di}$).

Maximal volitional inspiratory maneuver. Three maximal volitional inspiratory maneuvers were performed initially: maximal inspiratory effort against an occluded mouthpiece (a Mueller maneuver) from functional residual capacity to determine maximal inspiratory mouth pressure (PI_{max}), maximal sniff, and maximal inspiration to total lung capacity.[5] These maneuvers were performed sitting upright in a chair with a nose clip in place and were repeated several times to ensure maximal volitional effort.

P_{di} parameters. LabChart data were exported as Matlab files and analyzed offline in the widely available Matlab R2014a software. Transdiaphragmatic pressure-time product (PTP_{di}), the time-integral of P_{di},[6,8] was calculated for each respiratory cycle by multiplying the area under the curve of the inspiratory P_{di} signal by the respiratory frequency (reported in $cmH_2O \cdot s^{-1} \cdot min^{-1}$). PTP_{di} was calculated after removal of the baseline from the inspiratory P_{di} signal, which was determined for each respiratory cycle as the minimum level observed from the start of inspiration to the start of expiration (i.e., between points of zero flow).

Quantification of diaphragm electromyography. Diaphragm electromyography (EMG_{di}) signals were analyzed offline on a laptop running LabChart software (Version 7.2, ADInstruments Pty). An adaptive mains filter was applied and an additional band-pass filter between 20–1000 Hz was applied to EMG_{di} signals to reduce the P and T waves of electrocardiographic artifacts and the low-frequency, large amplitude deflections in signal baseline produced by electrode motion and esophageal peristalsis. EMG_{di} signals were converted to root mean square (RMS) using a moving window of 50 ms. The RMS peak values of EMG_{di} were then determined by manually analyzing inspiratory EMG_{di} signal segments falling between QRS complexes of the electrocardiographic noise. For each respiratory cycle, the highest value obtained across all bipolar electrode pairs was selected (peak RMS EMG_{di}). As previously described,[5] the per-breath RMS peak values of EMG_{di} were expressed as percentages of the largest RMS peak value of EMG_{di} obtained during the three maximal volitional maneuvers (EMG_{di}%max).

Electrical Impedance Tomography Measurements

Electrical impedance tomography (EIT) can be used to monitor regional ventilation with a high temporal resolution.[2] In this study, EIT data were recorded with the Goe-MF II EIT device (CareFusion, Höchberg, Germany). The 16 electrodes were placed in a cross-sectional plane circumferentially around the thorax, 5 cm below the fifth intercostal space (see **Fig. A1**), and generated 33 topographical images per second. Goe-MF II uses the adjacent measurement pattern to acquire an EIT frame. Two EIT frames are used to reconstruct the change of regional impedance over time. In this study, tidal breathing at +1 G_x was used as a baseline measurement and all EIT images show the impedance change compared with this reference. The overall change of impedance during tidal breathing is proportional to the tidal volume.[3] The regional contribution of different lung regions to ventilation can be quantified with functional EIT (fEIT) images. These images are calculated from a series of EIT images, where each pixel shows the standard deviation of a pixel from the series. The reconstruction and the fEIT image calculation were performed with the Dräger EIT Data Analysis Tool 6.1 (Dräger Medical, Lübeck, Germany). The posterior regions (P1–P4) of the lung were considered the dependent region and the anterior regions (A1–A4) were considered nondependent. Regional distribution in tidal ventilation derived from tidal impedance was expressed as a percentage of the global tidal impedance change (i.e., the sum impedance change across all regions of interest).

Video and Procedure for Arterial Blood Sampling on the Centrifuge

Link to online video: https://media.kcl.ac.uk/media/Arterial±blood±sampling±on±a±human±centrifuge/0_ryhm1umn.

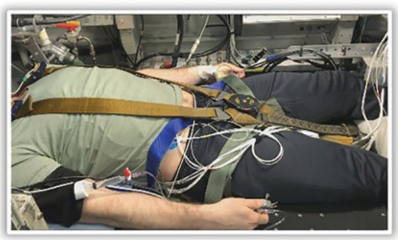

Arterial blood sampling on a human centrifuge; © Dr. Thomas Smith, Head of Aerospace Medicine Research, King's College London; https://www.kcl.ac.uk/people/thomas-smith.

Description of procedure. The above link provides a video of the procedure for arterial blood sampling on the centrifuge. The video was taken while the centrifuge was stationary, but samples were taken during high-G acceleration while the centrifuge was spinning. The arterial cannula is in the left radial artery. The subject holds two pre-evacuated syringes, one in each hand, which are attached to the arterial line via three-way taps (all Luer locking connections). To take a sample, first the right-hand syringe is opened to draw back the flush saline in the arterial line. The left-hand syringe is then opened to take the arterial blood sample. Both syringes are then closed and the line is flushed by pulling the toggle on the Springfusor (Go Medical Industries, Perth, Australia) with the right hand. The sample is retrieved and analyzed by the research team as soon as the centrifuge comes to a stop. Blood analysis was performed in duplicate using a point-of-care analyzer (iSTAT-1, Abbott Point of Care Inc., Abbott Park, IL, USA).

SUPPLEMENTAL REFERENCES

1. Baydur A, Behrakis PK, Zin WA, Jaeger M, Milic-Emili J. A simple method for assessing the validity of the esophageal balloon technique. Am Rev Respir Dis. 1982; 126(5):788–791.
2. Frerichs I, Amato MB, van Kaam AH, Tingay DG, Zhao Z, et al. Chest electrical impedance tomography examination, data analysis, terminology, clinical use and recommendations: consensus statement of the TRanslational EIT developmeNt stuDy group. Thorax. 2017; 72(1):83–93.
3. Frerichs I, Hahn G, Hellige G. Thoracic electrical impedance tomographic measurements during volume controlled ventilation-effects of tidal volume and positive end-expiratory pressure. IEEE Trans Med Imaging. 1999; 18(9):764–773.
4. Jolley CJ, Luo YM, Steier J, Rafferty GF, Polkey MI, Moxham J. Neural respiratory drive and breathlessness in COPD. Eur Respir J. 2015; 45(2):355–364 https://doi.org/10.1183/09031936.00063014. PubMed
5. Jolley CJ, Luo YM, Steier J, Reilly C, Seymour J, et al. Neural respiratory drive in healthy subjects and in COPD. Eur Respir J. 2009; 33(2):289–297.
6. Kyroussis D, Polkey MI, Hamnegard CH, Mills GH, Green M, Moxham J. Respiratory muscle activity in patients with COPD walking to exhaustion with and without pressure support. Eur Respir J. 2000; 15(4):649–655.
7. Luo YM, Moxham J. Measurement of neural respiratory drive in patients with COPD. Respir Physiol Neurobiol. 2005; 146(2–3):165–174.
8. Marini JJ, Smith TC, Lamb VJ. External work output and force generation during synchronized intermittent mechanical ventilation. Effect of machine assistance on breathing effort. Am Rev Respir Dis. 1988; 138(5):1169–1179.
9. Quanjer PH, Stanojevic S, Cole TJ, Baur X, Hall GL, et al. Multi-ethnic reference values for spirometry for the 3-95-yr age range: the global lung function 2012 equations. Eur Respir J. 2012; 40(6):1324–1343.

10. Reilly CC, Ward K, Jolley CJ, Lunt AC, Steier J, et al. Neural respiratory drive, pulmonary mechanics and breathlessness in patients with cystic fibrosis. Thorax. 2011; 66(3):240–246.
11. Scano G, Innocenti-Bruni G, Stendardi L. Do obstructive and restrictive lung diseases share common underlying mechanisms of breathlessness? Respir Med. 2010; 104(7):925–933.
12. Watson AC, Hughes PD, Louise Harris M, Hart N, Ware RJ, et al. Measurement of twitch transdiaphragmatic, esophageal, and endotracheal tube pressure with bilateral anterolateral magnetic phrenic nerve stimulation in patients in the intensive care unit. Crit Care Med. 2001; 29(7):1325–1331.

SUPPLEMENTARY RESULTS

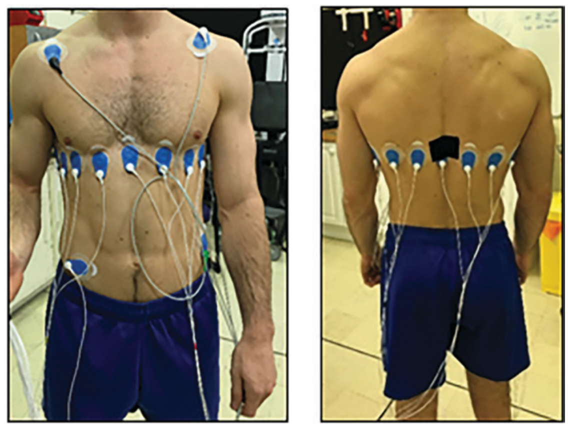

Fig. A1. Placement of electrical impedance tomography electrodes.

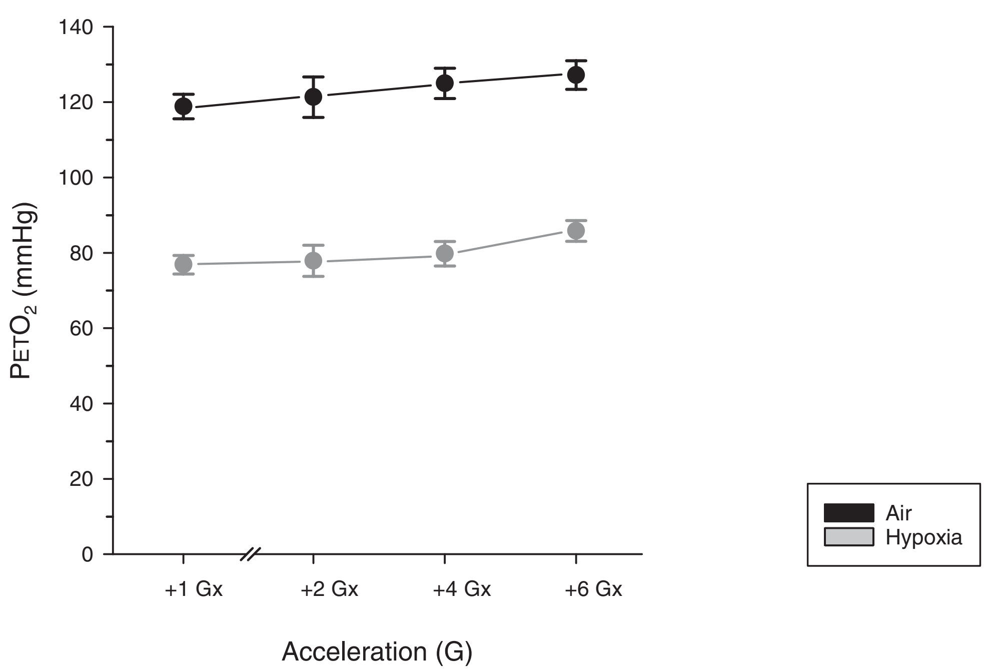

Fig. A2. End-tidal partial pressure of oxygen. Data were obtained while breathing air (black symbols) and breathing 15% oxygen to simulate a cabin pressure altitude of 8000 ft (2438 m; gray symbols). End-tidal partial pressure of oxygen ($P_{ET}O_2$) was significantly lower breathing 15% oxygen [$F(1,7) = 1552.5$, $P < 0.001$] and there was a small increase in $P_{ET}O_2$ with increasing $+G_x$ [$F(2.3,16.1) = 5.5$, $P = 0.013$; repeated measures ANOVA with Greenhouse-Geisser correction]. Data are mean ± SEM.

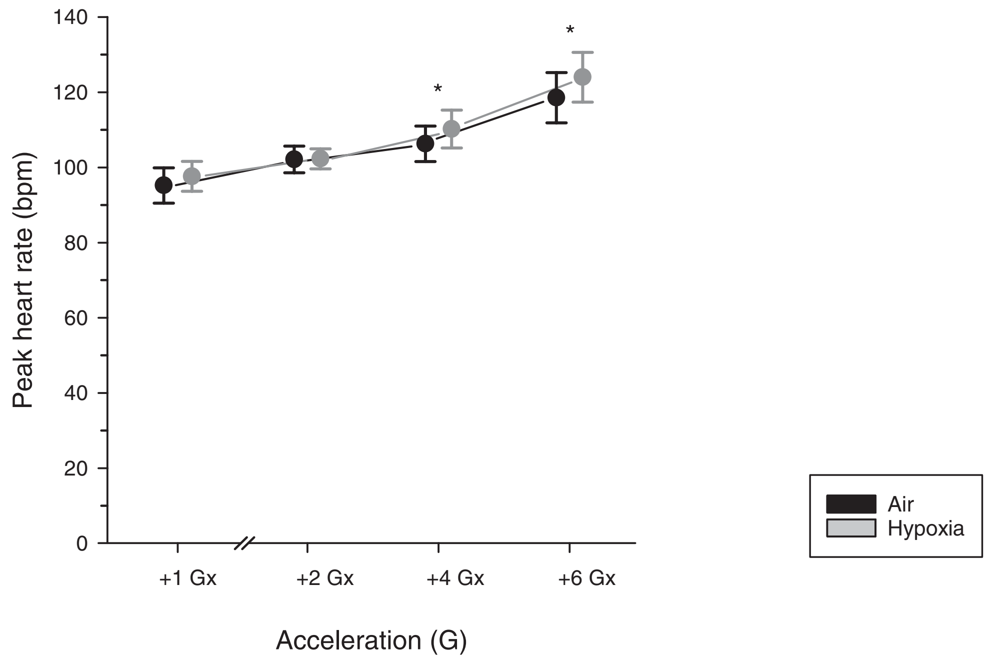

Fig. A3. Peak heart rate. Data were obtained while breathing air (black symbols) and breathing 15% oxygen to simulate a cabin pressure altitude of 8000 ft (2438 m; gray symbols). The effect of increasing $+G_x$ was statistically significant [$F(1.5,15.1) = 17.3$, $P < 0.001$]. Breathing 15% oxygen had no significant effect. Asterisks denote a statistically significant difference ($P < 0.05$) from baseline for respective G loads after Bonferroni adjustment for multiple comparisons. Data are mean ± SEM.

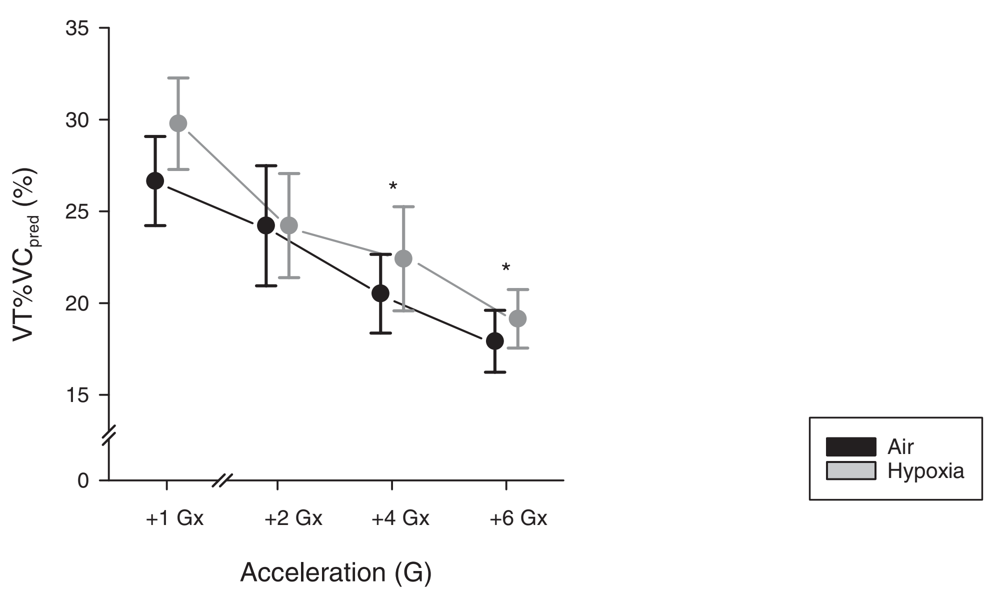

Fig. A4. Tidal volume normalized to predicted vital capacity. Tidal volume was normalized to predicted vital capacity to account for variation in age, size, height, and ethnicity of subjects. Tidal volume is reported as a percentage of the predicted value for vital capacity ($VT\%VC_{pred}$) with predicted values derived from the Global Lung Function Initiative.[9] Data were obtained while breathing air (black symbols) and breathing 15% oxygen to simulate a cabin pressure altitude of 8000 ft (2438 m; gray symbols). The effect of increasing $+G_x$ was statistically significant [$F(2.6,21.0) = 10.5$, $P < 0.001$]. Breathing 15% oxygen had no significant effect. Asterisks denote a statistically significant difference ($P < 0.05$) from baseline for respective G loads after Bonferroni adjustment for multiple comparisons. Data are mean ± SEM.

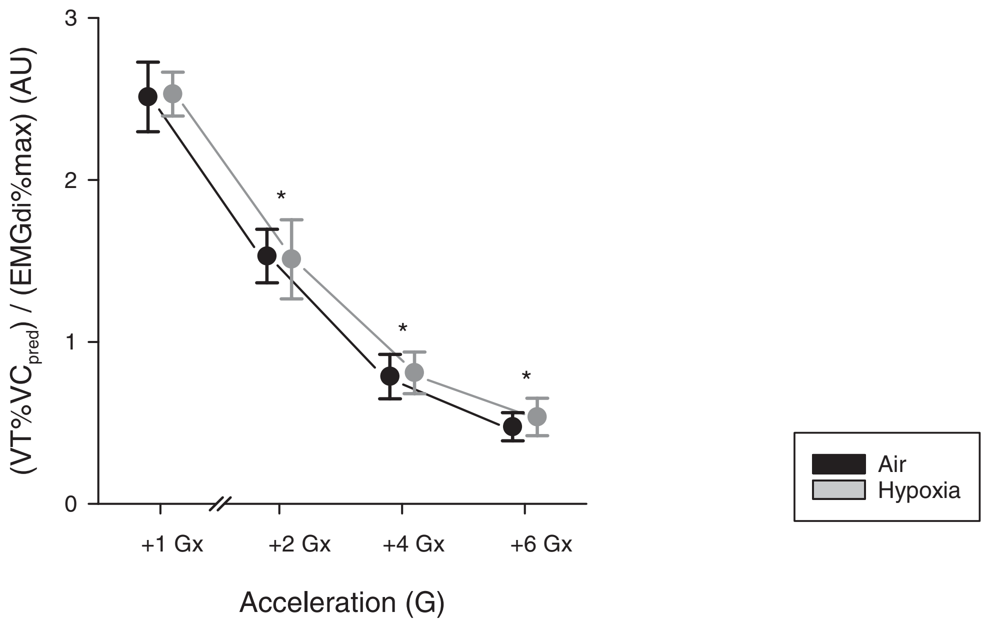

Fig. A5. Quantitative index of neuroventilatory uncoupling. Breathlessness increases disproportionally if ventilatory responses are limited by impaired pulmonary mechanics, which is termed neuroventilatory uncoupling.[11] A quantitative index of neuroventilatory uncoupling was calculated as the ratio of normalized tidal volume and neural respiratory drive.[4,5] Tidal volume was normalized to predicted vital capacity ($VT\%VC_{pred}$, reported in Fig. A4). Neural respiratory drive was determined from diaphragm electromyography (EMG_{di}) as the proportion of maximum volitional EMG_{di} ($EMG_{di}\%max$). The resultant neuroventilatory uncoupling index, $(VT\%VC_{pred})/(EMG_{di}\%max)$, is reported in arbitrary units (AU) and decreased significantly with increasing $+G_x$ to values below those reported in patients with chronic obstructive pulmonary disease [$F(2.0,15.6) = 193.8$, $P < 0.001$].[5] Data were obtained while breathing air (black symbols) and also while breathing 15% oxygen to simulate a cabin pressure altitude of 8000 ft (2438 m; gray symbols), which did not significantly affect neuroventilatory uncoupling. Asterisks denote a statistically significant difference ($P < 0.05$) from baseline for respective G loads after Bonferroni adjustment for multiple comparisons. Data are mean ± SEM.